Scanning tunneling microscopy, high-resolution electron energy loss spectroscopy, and theoretical studies of trimethylphosphine (TMP) on a Si(111)-(7×7) surface

Y. Fukuda [a],[*], M. Shimomura [a], G. Kaneda [a], N. Sanada [a], V.G. Zavodinsky [b], I.A. Kuyanov [b], E.N. Chukurov [b]

[a] Research Institute of Electronics, Shizuoka University, Hamamatsu 432-8011, Japan
[b] Institute for Automation, Far Eastern Branch of the Russian Academy of Sciences 5 Radio, 690041, Vladivostok, Russia and Far Eastern State University, 8 Sukhanova, 69022, Vladivostok, Russia

Abstract

Adsorption of trimethylphosphine (TMP) on a Si(111)-(7×7) surface was studied using scanning tunneling microscopy (STM), high-resolution electron energy loss spectroscopy (HREELS), and theoretical calculations. It was found from STM and HREELS that most of the TMP molecules are adsorbed molecularly on center adatom sites at room temperature. A semi-empirical calculation (AM1 method) verified that this is energetically favorable. It is also found that one of the protrusions (unoccupied state images) on the center adatom site moves to the rest atom site and three protrusions (occupied state images) appear on the corner and center adatom sites in the second scan (interval of a few minutes). The results of a theoretical calculation indicate that adsorption of the three CH_3 groups and the P atom on the adatom and rest atom sites, respectively, is energetically favorable. This explains the STM images well. The HREELS result suggests that the CH_3 group is split off and dissociated into CH_2 (or CH) and H upon heating the sample. The result of the theoretical calculation shows that the dissociation of CH_3 into CH_2 and H is energetically preferable when CH_2 is bridged between an Si adatom and an Si atom in the second layer and H is on the rest atom site. © 1999 Elsevier Science B.V. All rights reserved.

1. Introduction

Adsorption, decomposition, and surface reaction of gases have been widely studied on semiconductor surfaces because they are very important for not only basic science but also for device applications. Recently fabrications of nanometer scale structures and atomically controlled devices (such as quantum dots and wires, superlattices, etc.) have been developed using metalorganic chemical vapor deposition (MOCVD) and chemical beam epitaxy (CBE). The first step in the fabrication of the structures and devices is adsorption and decomposition of metalorganic compounds as precursors in MOCVD and CBE. From the above point of view, many studies of the adsorption and decomposition of the precursors

* Corresponding author. Fax: +81-53-4781651.
E-mail address: royfuku@ipc.shizuoka.ac.jp (Y. Fukuda)

on the semiconductor substrates have been reported [1].

Since scanning tunneling microscopy (STM) can image an individual atom on surfaces in certain electronic states, many studies have been reported on well-defined surfaces. In particular, an Si(111)-(7×7) surface is very interested because Si adatoms with several different electronic states coexist on the reconstructed surface. Therefore, it is expected that molecules adsorb and decompose on specific sites. For examples, it has been reported that C_2H_2 [2] and $AlCl_3$ [3] are adsorbed preferentially on the center adatom sites whereas PH_3 and NH_3 are adsorbed on the rest atom sites [4–6]. It was found that trimethylphosphine (TMP) [$(CH_3)_3P$], which is one of the useful precursors for phosphorus in MOCVD, adsorbs preferentially on the center adatom sites and that most of the molecules adsorbed on the corner adatom sites migrate to the center adatom sites after a few minutes [7].

In this work three protrusions arranged in a triangular shape are found in STM images when the TMP molecule migrates from the center adatom site to the rest atom site. The STM image, however, cannot distinguish the atoms and molecules on the surfaces. Therefore, we studied the adsorption and decomposition of TMP on the Si(111)-(7×7) surface in detail using high-resolution electron energy loss spectroscopy (HREELS). Theoretical calculations were also performed to clarify the experimental results.

2. Experimental

An n-type (phosphorus-doped) Si(111) sample (~2 Ω cm) was used for the experiments. It was resistively heated at 1523 K to remove surface oxides. The cleanness of the (7×7) surface was confirmed by Auger electron spectroscopy (AES), low-energy electron diffraction (LEED), and STM. After the clean sample had been exposed to 1 L (=10^{-6} Torr s) TMP gas in the preparation chamber, it was transferred to an analytical chamber. STM measurements were carried out at 1.5 and −1.5 V (sample bias) at constant currents.

The scanning tunneling microscope (JSTM-

4500XT, JEOL) is mounted in an ultrahigh vacuum chamber (base pressure, below 1×10^{-10} Torr) with a preparation chamber. LEED and AES facilities, an sputter ion gun, and a gas inlet line are installed in the preparation chamber.

An HREELS apparatus, which was built by ourselves, was used to examine chemical species on the surface exposed to TMP. A typical resolution was about 10 meV. The HREELS spectra were measured after the sample had been exposed to TMP at 110 and 300 K, and subsequently annealed at various temperatures.

3. Experimental results and discussion

Fig. 1 shows STM unoccupied (Fig. 1a,c) and occupied (Fig. 1b,d) state images for the Si(111)-(7×7) surface exposed to TMP at RT. The images were measured in the first (Fig. 1a,b) and second (Fig. 1c,d) scans (interval of about a few minutes) of the same area. Five bright protrusions are seen in the unoccupied state images (Fig. 1a), where the protrusions are on the center adatom sites. This is consistent with the previous result that most (about 88%) of the protrusions are on the center adatom site [7]. One (arrow) of them becomes less bright for the unoccupied state images (Fig. 1c) than that in Fig. 1a. A similar less bright protrusion is seen on the right-hand side in Fig. 1a. The less bright protrusions are found to be located on the rest atom site. In contrast, the protrusion (arrow in Fig. 1b) in the occupied state images changes into the three in Fig. 1d. Similar protrusions are also seen on the right-hand side in Fig. 1b. The number of the groups of three protrusions arranged in a triangular shape is low at 300 K. Their number increased at elevated temperature. One (the corner adatom site) of the three is brighter than the others.

A cross-sectional plot along the line (between the corner holes) in Fig. 1a is shown in Fig. 2. Five peaks are found in the plot. D and E correspond to the center adatom sites (in the unfaulted half unit cell) without adsorption of TBP. A, C, and B correspond to the corner and center adatom and rest atom sites (in the faulted half unit cell)
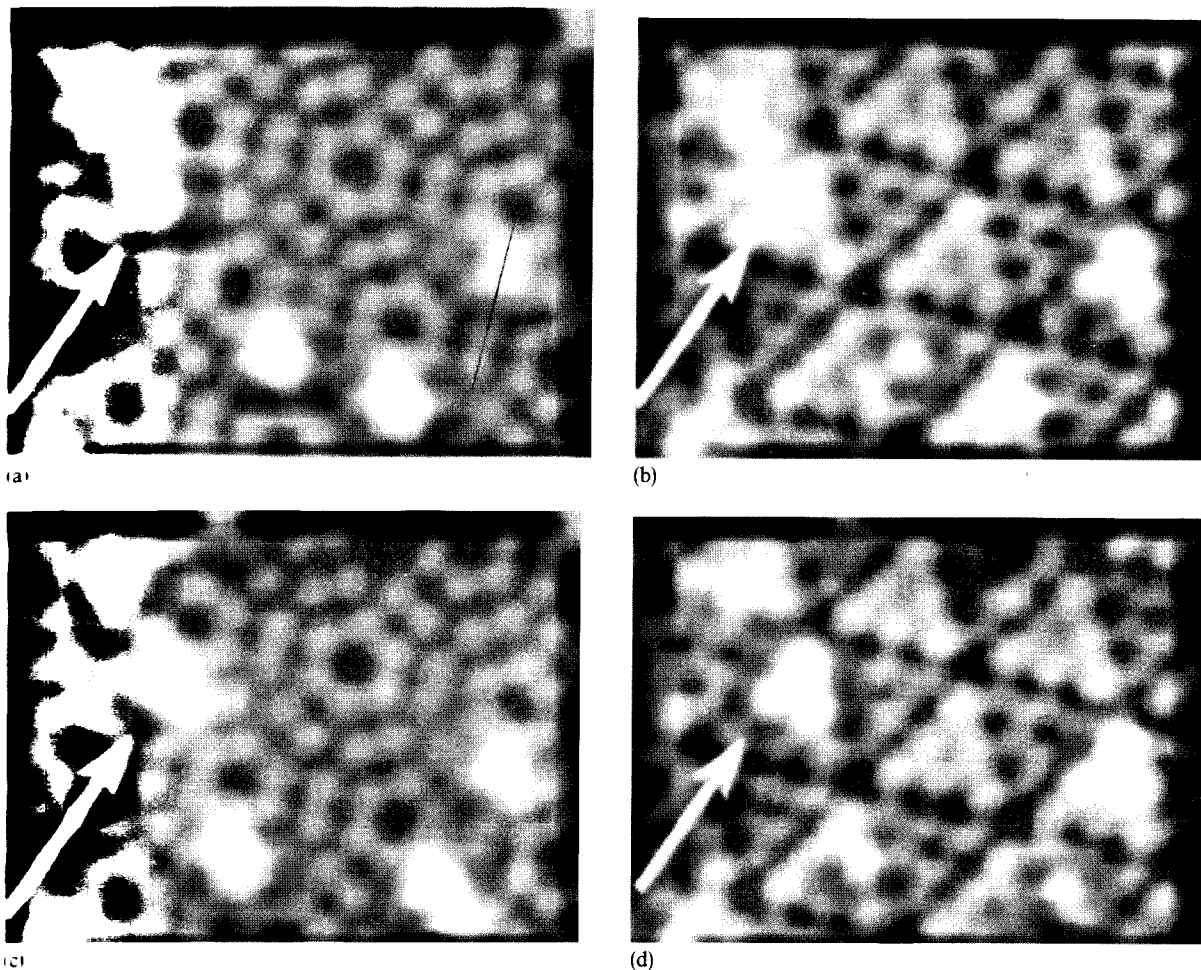
Fig. 1. STM unoccupied (a,c) and occupied (b,d) state images for the Si(111)-(7×7) surface exposed to TMP (1 L) at room temperature (RT) measured at bias voltages of 1.5 and −1.5 V, respectively. The images were measured in the first (a,b) and second (interval of about a few minutes) (c,d) scan of the same area.

respectively. A, B, and C are higher than D and E, which is due to adsorption of CH_3 (A and C) and P (B). This will be discussed later.

Since the intensity of HREELS spectra for the Si(111)-(7×7) surface exposed to the TBP gas (1 L) was weak, the HREELS measurements were carried out on the sample exposed to 30 L and 6 L of **TBP**. Comparison of the STM image for the surface exposed to 1 L with those for 30 L and 6 L indicated that all are essentially the same except for the number of the adsorbed TBP molecules. The HREELS spectra of the Si(111)-(7×7) surface exposed to TMP (30 L) at 110 K (a) and

subsequently heated at 270 K (b) are displayed in Fig. 3. Sharp vibration peaks are found at 2930, 1410, and 938 cm^{-1} and shoulders at about 1282 and 706 cm^{-1}. They can be ascribed to $v(CH_3)$, $\delta_a(CH_3)$, $\rho_r(CH_3)$, $\delta_s(CH_3)$, and $v_a(PC)$ [8–10], where v, δ_a, ρ_r, δ_s, and v_a correspond to stretching, asymmetric deformation, rocking, symmetric deformation, asymmetric stretching vibrations. Most of the peaks do not change in wavenumber except $v_a(PC)$ at 270 K where a weak peak appears at 683 cm^{-1}. Since a multilayer of TMP is formed at 110 K and the **TMP** would be chemisorbed with P at 270 K [11], the $v_a(PC)$ and
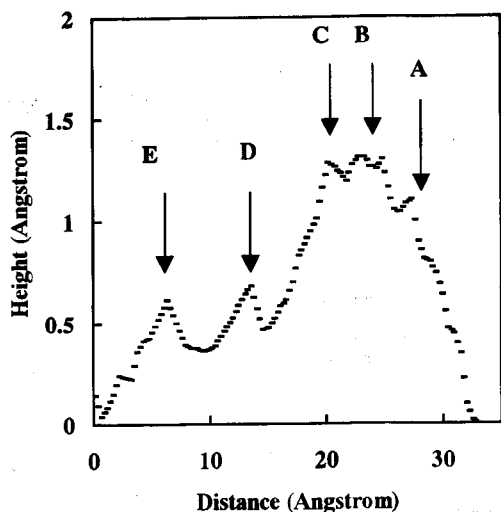
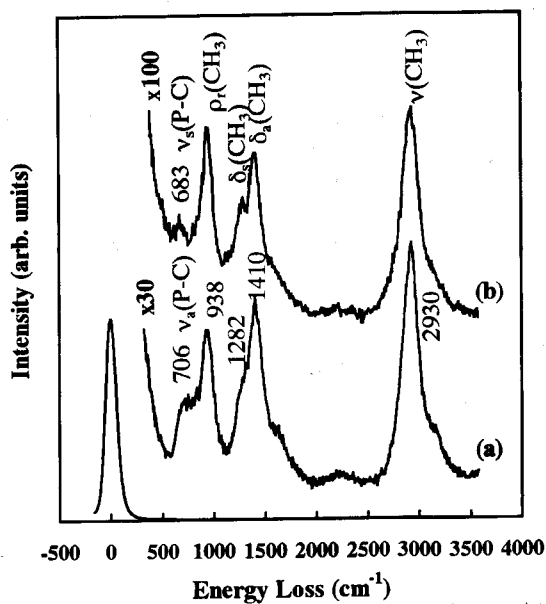Fig. 2. Cross-sectional plot along the line (between the corner holes) in Fig. 1a.

Fig. 3. HREELS spectra of the Si(111)-(7 × 7) surface exposed to TMP (30 L) at 110 K (a) and subsequently heated at 270 K (b).

$v_s(PC)$ peaks are observable at 110 and 270 K, respectively, as observed on a Pt(111) surface [11]. The broad peak at about 2219 cm^{-1} and a shoulder at about 1640 cm^{-1} would be combination bands of $\delta_a(CH_3)+\rho_r(CH_3)$ and $v_a(PC)+\rho_r(CH_3)$,

respectively. The shoulder at about 3188 cm^{-1} would be due to the combination band of $v(CH_3)$ with a low wavenumber mode which is superimposed on an intense elastic peak.

HREELS spectra of TMP (6 L) on the Si(111)-(7 × 7) surface annealed at various temperatures are shown in Fig. 4. Clear vibration peaks at 2960, 1416, and 952 cm^{-1} are found in Fig. 4a. They correspond to $v(CH_3)$, $\delta_a(CH_3)$, and $\rho_r(CH_3)$, respectively, although the wavenumbers are higher than those in Fig. 3b. This would be due to the isolated TMP molecule chemisorbed on the surface. Shoulders at about 1280 and 700 cm^{-1} are also seen. The presence of the latter band indicates that most of the CH$_3$ group is bonded to the P atom at 300 K. Upon heating the sample at 400 K, a new peak appears at 2070 cm^{-1}. The 2960 and 952 cm^{-1} peaks are shifted to 2928 and 864 cm^{-1}, respectively, at 500 K and the 2070 cm^{-1} peak increases in intensity. The 2070 cm^{-1} peak can be ascribed to $v(SiH)$ [12] which is due to dissociation
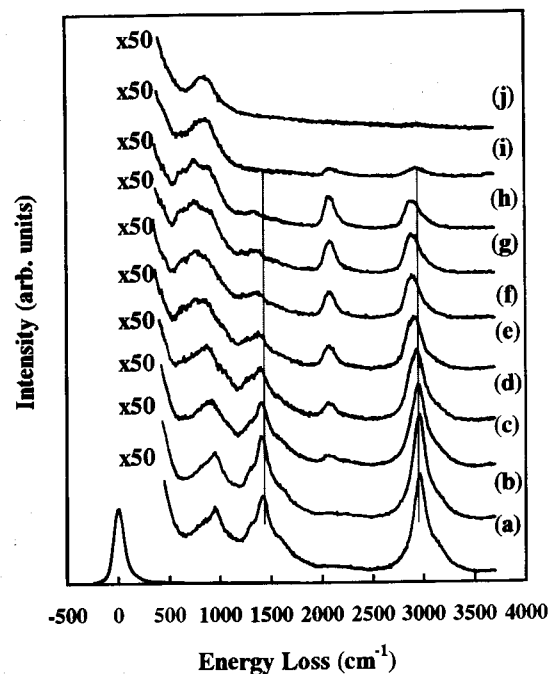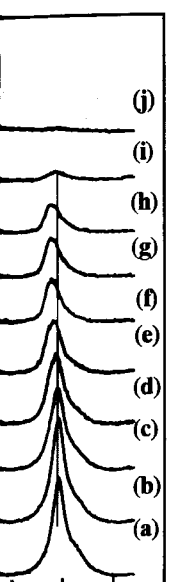

Fig. 4. HREELS spectra of the Si(111)-(7 × 7) surface exposed to TMP (6 L) at 300 K (a) and subsequently heated at 350 (b), 400 (c), 500 (d), 600 (e), 700 (f), 800 (g), 900 (h), 1000 (i), and 1200 K (j).

about 3188 cm⁻¹
n band of $v(CH_3)$
which is superim-

L) on the Si(111)-
ious temperatures
ion peaks at 2960,
in Fig. 4a. They
), and $\rho_r(CH_3)$,
umbers are higher
uld be due to the
orbed on the sur-
and 700 cm⁻¹ are
tter band indicates
bonded to the P
e sample at 400 K,
⁻¹. The 2960 and
)28 and 864 cm⁻¹,
2070 cm⁻¹ peak
cm⁻¹ peak can be
due to dissociation

(j)
(i)
(h)
(g)
(f)
(e)
(d)
(c)
(b)
(a)

500 3000 3500 4000

m⁻¹)

(7×7) surface exposed
ntly heated at 350 (b),
(g), 900 (h), 1000 (i),

of the CH_3 group. The full width at half-maximum (FWHM) of the peak at about 2928 cm⁻¹ increases at 400 and 500 K. This implies that the CH_3 group bonded to the phosphorus atom is changed in the vibration mode. Two possible ... would occur: one is the splitting-off of the methyl group bonded to the P atom (electronegativity = 2.1) to Si (1.7) and the other is the formation of CH_x ($x = 1$ and 2) on the surface. The former and the latter lead to a decrease [13] and an increase [14] in the wavenumber of $v(C-H)$, respectively, resulting in increase in the FWHM of the 2070 cm⁻¹ peak. The splitting-off also decreases the wavenumber of $\delta_a(CH_3)$ owing to the low electronegativity of the Si atom [14], which is in good agreement with the result that the 1416 cm⁻¹ peak is shifted to 1392 cm⁻¹ at 500 K. Since the 2070 cm⁻¹ peak is observed between 400 and 900 K, both the splitting-off and the formation of CH_x would occur. The $v(SiH)$ peak and 640 cm⁻¹ band, which can be assigned to $\delta(SiH)$ [12], increase to 900 K. The feature in the spectral change between 600 and 900 K is that the new peak appears at about 760 cm⁻¹ and that the 1410 and 2960 cm⁻¹ peaks are shifted to 1390–1340 and 2930–2890 cm⁻¹, respectively. Since $v(CH_2)$, $\delta(CH_2)$, and $\rho(CH_2)$ modes were observed at about 2900, 1362–1382, and 776–745 cm⁻¹ for $SiH_3CH_2SiH_3$ [15] and $GeH_3CH_2SiH_3$ [16], the above feature would be due to formation of CH_2 species on the surface. Similar peaks have been found in the decomposition of trimethylgallium on GaAs(001) [17]. The $v(CH)$, $\delta_{as}(CH)$, $\rho_{as}(CH)$, and $\rho_s(CH)$ modes were found at 2890, 1315, 970, and 730 cm⁻¹, respectively on the Si(111)-(7×7) surface exposed to acetylene [18]. Since they are superimposed on the bands between about 500 and 1350 cm⁻¹ in Fig. 4d–h, it is not clear that the CH species are formed on the surface. The $v(SiC)$ peak [19] is observed at about 850 cm⁻¹ at 1200 K. The weak shoulder at about 500 cm⁻¹, which can be ascribed to $v(SiP)$ [20], is seen between 600 and 1000 K although it is superimposed on a steep background. This is consistent with the result that P atoms are desorbed from the Si(111)-(7×7) surface at about 1000 K [20]. The species $P(CH_3)_3$, $P(CH_3)_2$, and $P(CH_3)$ are not distinguished because of a limited resolution [8,9,21].

The HREELS result showed that most of the CH_3 groups are bonded to the P atom at 300 K. However, taking account of the result that the splitting-off of the CH_3 group, the formation of CH_x, and the increase in the number of the three protrusions are found at elevated temperature (above 400 K), the three protrusions in Fig. 1d would be the decomposition products CH_3 (or CH_x) and P.

4. Method of calculation and its verification

To study the energetics and geometry of the TMP molecule on the Si(111)-(7×7) surface, we used the advanced semi-empirical quantum-chemical AM1 method (Austin Model 1) [22]. This is a version of the modified intermediate neglect of differential overlap (MINDO) [23–25] realized in the frame of the CLUSTER-Z1 package [26,27]. This package allows us to optimize atomic configurations by minimizing the total energy gradients over all atomic coordinates. The calculation speed with the semi-empirical method is significantly greater than that with the ab initio method, but its accuracy depends strongly upon choosing the correct set of parameters. In particular, the AM1 method is usually parameterized to reproduce heats of atomization and molecular geometry. Therefore, the ability of the semi-empirical method to describe an arbitrary configuration of atoms must be verified. The AM1 method was recently verified for a silicon–phosphorus system [28,29] where $P-Si$ and $P-P$ bonds on the Si(100) surface were studied. It was found that the $P-Si$ bonds are energetically preferable, which is in accordance with the STM result [30,31] and ab initio molecular orbital calculations [30]. All quantitative values (energy differences, bond lengths and angles) close to the known data [30,31] have been obtained. Before studying the TMP molecule on the Si(111)-(7×7) surface, test calculations of the TMP molecular geometry were carried out. A schematic structure of the TMP molecule is shown in the upper part of Fig. 5 and the calculated parameters for TMP in this work are compared with the result obtained by an ab initio Hartree–Fock calculation [32] (Table 1). The AM1 method

Trimethylphosphine
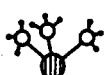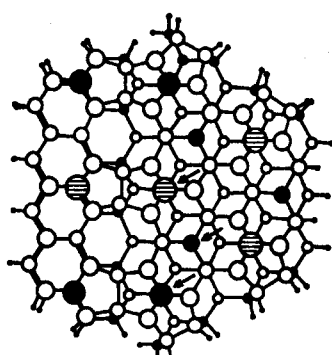
① **phosphorus**

○ **carbon**

· **hydrogen**

Si (111)-(7x7) substrate

⊜ **center adatom**

● **corner adatom**

○ **1st layer**

○ **2nd layer**

● **rest atom**

· **3rd layer**

○ **4th layer**

· **hydrogen**

Fig. 5. Schematic illustrations of the TMP molecule and the $Si_{145}H_{75}$ cluster modeled for the Si(111)-(7 × 7) surface. The circles (arrow) correspond to atoms (the rest atom, center and corner adatom sites) used as adsorption sites in the calculations.

Table 1
Geometry of the TMP molecule

	P—C bond distance (Å)	C—H bond distance (Å)	C—P—C angle (°)
Our result	1.76	1.11	100.90
Hartree–Fock calculations	1.845	1.096	98.95

gives us a good accuracy for the calculations of the TMP molecule.

5. Theoretical results and discussion

The STM experiment indicated that the behaviors in adsorption and migration of the TMP molecule on the unfaulted and faulted regions of the (7 × 7) surface are similar [7]. Therefore, only the TMP molecule on the unfaulted region is studied. The $Si_{145}H_{75}$ cluster shown in Fig. 5 is used as a model of the Si(111)-(7 × 7) surface (the

unfaulted region) for our calculation. This cluster consists of four atomic layers and eight adatoms. All broken Si bonds were terminated by H atoms with the equilibrium Si—H distance, 1.46 Å. The initial Si coordinates were taken from the reported data [33] and then the cluster geometry was optimized by the AM1-CLUSTER-Z1 procedure. No symmetry restrictions were adopted in our calculation. The final atomic positions are in agreement with the previous data [33] within ±0.05 Å.

To study the energetics of the TMP adsorption on the Si(111)-(7 × 7) surface, the TMP molecule was placed on three different sites: on the rest atom, the center and the corner adatom sites. These sites are marked by arrows in Fig. 5. The binding energies (BE) together with the P—Si and P—C bond lengths for the three cases are listed in Table 2. It is clear that the center adatom is a more favored site for the adsorption than the rest atom, which is in accordance with the experiment [7]. The BE for TMP on the center adatom site is lower by 0.09 eV than that on the corner adatom. From the experimental diagram of the distribution of adsorption sites [7], one can obtain the energy difference of 0.06 eV, which is in good agreement with the calculated result.

The rest atom is surrounded by three neighboring adatoms with dangling bonds. Each center and corner adatom is located close to two and one neighboring rest atoms, respectively. For dissociation of the TMP molecule, assuming that the P atom and three CH_3 groups adsorb on the rest atom and the adatom sites, respectively, the BE is found to be −2.67 eV which is lower by about 1 eV than that in the molecular adsorption. In other words, the dissociation of the TMP molecule on the rest atom is energetically possible. This can explain the STM result that the three bright protru-

Table 2
Binding energy and geometry parameters of the TMP molecule placed on the various sites of the Si(111)-(7 × 7) surface

Site	Binding energy (eV)	P—Si distance (Å)	P—C distance (Å)
Center adatom	−1.94	2.38	1.77
Corner adatom	−1.85	2.38	1.77
Rest atom	−1.68	2.42	1.78

sions (occupied state image) appear on the adatom sites and new one (unoccupied state image) on the rest atom site after the second scan (Fig. 1c and d). In this case the P—Si distance is 2.42 Å and the C—Si distance is 1.85 and 2.08 Å for the center and corner adatom sites, respectively.

To make clear the changes in the STM images after the second scan, the calculation of the electronic structures for the TMP dissociated on Si(111)-(7 × 7) has been carried out assuming the same above configuration. Since the AM1 method does not correctly describe silicon electronic states (it gives, for example, a forbidden gap of several eV), we used here the ab initio local density method (the so-called discrete variation cluster version) in a cluster approach [34]. The cluster size was 50: $Si_{18}H_{19} + PC_3H_9$. Calculated partial densities of states for P and CH_3 adsorbed on the various sites are plotted in Fig. 6. One can see that the CH_3 groups have peaks of occupied states between the Fermi level and −1.5 eV. The phosphorus atom also has some states near −1.5 eV.
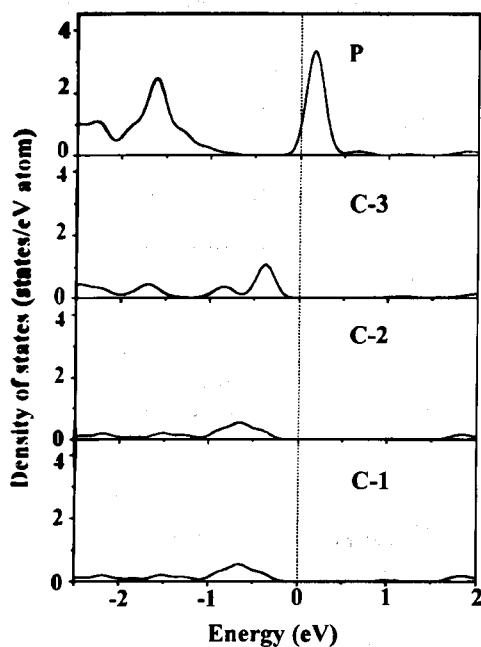

Fig. 6. Partial densities of states of P on the rest atom site and CH_3 on the adatom sites. C-1 (C-2) and C-3 correspond to CH_3 on the center and corner adatom sites. The vertical dotted line represents the Fermi level position.

However, the CH_3 is located higher above the silicon atom than the P atom: the CH_3 on the corner and center adatoms are higher by 0.91 and 0.72 Å, respectively, than the P atom on the rest atom. Thus, the CH_3–tip distances are less than the P–tip, leading to the result that the P–tip tunnel currents at $V_s = -1.5$ V should be lower. Furthermore, the CH_3 image on the corner adatom site must be brighter than that on the center adatom, which is in good agreement with the STM images. However, the phosphorus atom has an intense peak at +0.2 eV but the CH_3 groups have a very low density of unoccupied states between the Fermi level and +1.5 eV. Thus, the P image at $V_s = +1.5$ V is brighter than that of CH_3. However, the P-tip distance is large, resulting in the low image intensity. All these calculation results are in excellent agreement with the experimental data in Fig. 1.

In order to understand why the TMP molecule is not dissociated on the adatoms, the calculation was performed in the case where the P atom is on the center adatom and one of the three CH_3 groups adsorbs on the rest atom. The binding energy is found to be positive (+5.46 eV). This suggests that dissociation of TMP on the adatom sites is not favorable.

Moving the CH_3 groups away from the P atom and optimizing all other coordinates, the energy difference was calculated to obtain the dissociation reaction barrier. The result of the calculation is plotted as a function of the P—C distance in Fig. 7. A sharp barrier with a 5.3 eV height is found at the P—C distance, 2.3 Å. Although the energy corresponds to about 6×10^4 K, it would be less than that, taking account of a transition state for the dissociation reaction. For comparison, the dissociation energy of the free TMP molecule $[P(CH_3)_3 \rightarrow P + 3CH_3]$ was calculated. It is found to be 10.4 eV which is twice as high as the dissociation energy of TMP on the Si(111)-(7 × 7) surface.

The BE of the P atom on the rest atom site was calculated for the surface without the CH_3 group. The energy is found to be −0.77 eV. On replacing the P atom with the Si rest atom, a BE of −6.08 eV is obtained. The BE of the CH_3 group on the Si adatom is also found to be −2.95 eV. This implies
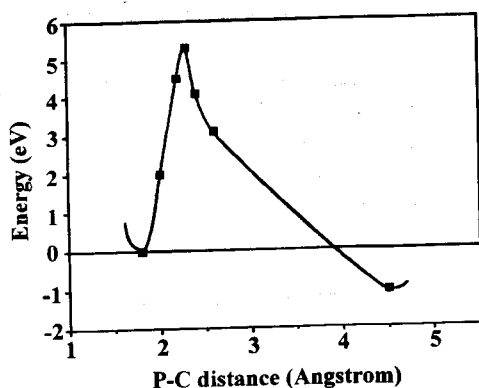
Fig. 7. The dissociation reaction barrier for the TMP molecule placed on the rest atom. The left minimum corresponds to the state in which the CH_3 group is bonded to the P atom. The right minimum corresponds to full dissociation (the CH_3 group is bonded to the Si adatom).
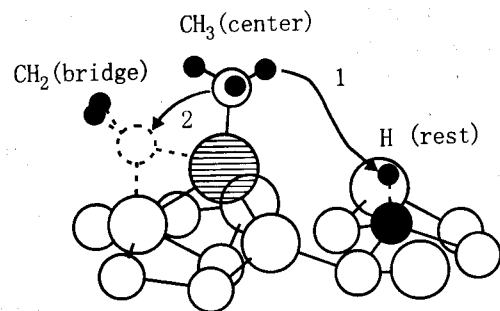

Fig. 8. Schematic view of the CH_3 (center)$\rightarrow CH_2$ (bridge)+H (rest) reaction on the Si(111)-(7×7) surface.

that the rest atom can be substituted by the phosphorus atom upon annealing, resulting in doping into the silicon substrate, while the CH_3 groups can be desorbed from the silicon surface when they are not dissociated. The latter is consistent with the experimental result (not shown here).

The BEs of CH_3, CH_2, and CH on the various sites were calculated to simulate the dissociation of the methyl group (Table 3). They are close, approximately from -2.4 to -2.9 eV. Thus, the H_xC-Si ($x=1-3$) bond energy is higher than that (-2.3 eV) of the Si$-$Si bond. The H$-$C bond energy in the CH_3 group on the center and corner adatom sites is -3.2 eV, while that in the free

CH_3 group is -3.62 eV. The H$-$Si bond energi for the H atom on the center, corner, and re atom sites are approximately -2.7 eV. Therefo the dissociation, $CH_3 \rightarrow CH_2 + H$, is not energe cally profitable. In fact, the total energy f ($CH_2 + H$) is higher by 0.5–0.6 eV than that f CH_3. However, the dissociation reaction may favorable if the H_2C-H bond breaking is accon panied by moving the CH_2 group to a bridge si between the Si adatom and one of the Si atoms the second layer (see Fig. 8 and Tables 4 and The result in Table 5 suggests that all configur tions for CH_2 (bridge)+H are energetical profitable. The most favorable configuration

Table 3
Binding energies of CH_3, CH_2, CH and H on the various sites of the Si(111)-(7×7) surface

Chemical species	Binding energy (eV)
CH_3 (center)	-2.52
CH_3 (corner)	-2.47
CH_2 (center)	-2.91
CH_2 (corner)	-2.77
CH (center)	-2.38
CH (corner)	-2.45
H in CH_3 (center)	-3.23
H in CH_3 (corner)	-3.24
H (center)	-2.70
H (corner)	-2.68
H (rest)	-2.69

Table 4
The total binding energy of $CH_2 + H$ on the various sites of Si(111)-(7×7) surface

Chemical species	Binding energy (e
CH_2 (center) + H (center)	-2.00
CH_2 (center) + H (corner)	-1.87
CH_2 (center) + H (rest)	-1.98
CH_2 (corner) + H (center)	-1.86
CH_2 (corner) + H (rest)	-1.95

Table 5
The total binding energy of CH_2 (bridge)+H on the vari sites of the Si(111)-(7×7) surface

Chemical species	Binding energy (e
CH_2 (corner, bridge) + H (center)	-2.61
CH_2 (corner, bridge) + H (rest)	-2.87
CH_2 (center, bridge) + H (center)	-2.93
CH_2 (center, bridge) + H (rest)	-3.24
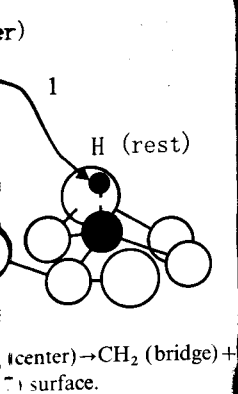
CH$_2$ (bridged between the center adatom and Si
at the second layer)+H (on the rest atom site).
This is calculated in detail. The calculation was
performed in two parts. First, the H atom was
moved away from the CH$_3$ in the rest atom
direction. The energy is plotted in Fig. 9a as a
function of the C—H distance. Second, the CH$_2$
group was moved to the bridge site in the following
way. The Si adatom—C bond was bent in the Si
adatom—C—Si atom (at the second layer) plane.
The result is shown in Fig. 9b. It is found that the

barrier height is rather high (approximately 3 eV)
at about 2 Å for the CH$_2$—H distance. In contrast,
the barrier is almost absent (only 0.08 eV) for the
bond bending of Si—CH$_2$ and the whole binding
energy of the (CH$_2$+H) complex reaches
−1.26 eV at 78° where CH$_2$ is at the bridge site.
The whole energy for the dissociation, CH$_3$
(center)→CH$_2$ (bridge)+H (rest), is −0.72 eV.
This is energetically favorable. This is also consis-
tent with the HREELS result although the adsorp-
tion site for the CH$_2$ cannot be distinguished in
the HREELS spectra.

Summarizing this work, adsorption of TMP on
the Si(111)-(7×7) surface has been studied by
STM, HREELS, and theoretical calculations. It
was found by STM that most of the TMP mole-
cules adsorb molecularly on the center adatom
sites at RT. It was verified by the semi-empirical
calculation (the AM1 method) that this is energeti-
cally favorable. After the second scan, one of the
protrusions (unoccupied state images) on the
center adatom site moved to the rest atom site and
three protrusions (occupied state images) appeared
on the corner and center adatom sites. The result
of the theoretical calculation indicates that adsorp-
tion of the three CH$_3$ groups and the P atom on
the adatom and rest atom sites, respectively, is
energetically favorable. This explains the STM
images well. The HREELS result suggests that the
CH$_3$ group is split-off and dissociated into CH$_2$
(or CH) and H upon heating the sample. The
energy for the dissociation reaction of CH$_3$ is
calculated in detail as a function of the C—H
bond length and of the Si—C angle. The result of
the calculation shows that the dissociation of
CH$_3$ into CH$_2$ and H is energetically preferable
when CH$_2$ is bridged between the Si center adatom
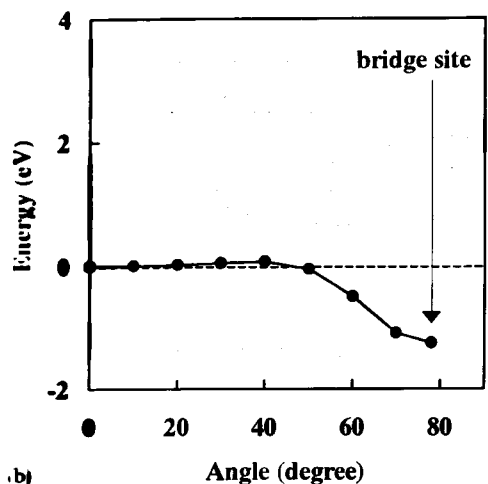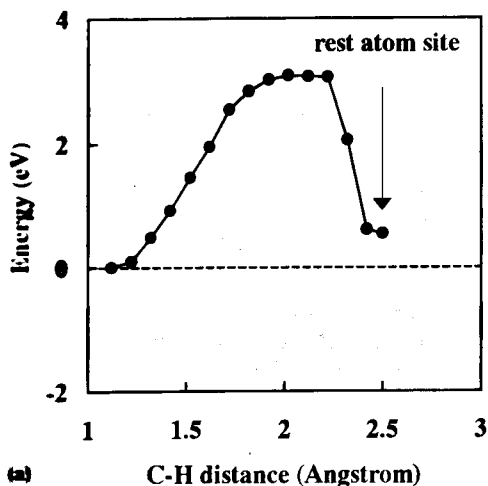and the Si atom in the second layer and H is on
the rest atom site.

Fig. 9. (a) Energy barrier for the H atom moving from CH$_2$
(center) to the rest atom site. (b). Energy barrier for CH$_2$
moving from the center adatom site to the bridge.

Acknowledgements

by the Russian Research Program 'Physics of Solid State Nanostructures'.

References

[1] A.C. Jones, CVD of Compound Semiconductors, CVH, Weinheim, 1997.

[2] J. Yoshinobu, D. Fukushi, M. Uda, E. Nomura, M. Aono, Phys. Rev. B 46 (1992) 9520.

[3] K. Uesugi, T. Takiguchi, M. Izawa, M. Yoshinobu, T. Yao, Jpn. J. Appl. Phys. 32 (1993) 6200.

[4] R. Wolkow, Ph. Avouris, Phys. Rev. Lett. 60 (1988) 1049.

[5] Ph. Avouris, R. Wolkow, Phys. Rev. B 39 (1989) 5091.

[6] P. Avouris, J. Phys. Chem. 94 (1990) 2246.

[7] M. Shimomura, N. Sanada, Y. Fukuda, P.J. Möller, Surf. Sci. 341 (1995) L1061.

[8] M. Halmann, Spectrochim. Acta 16 (1960) 407.

[9] J.D. Park, P.J. Hendra, Spectrochim. Acta, Part A 24 (1968) 2081.

[10] J.D. Park, P.J. Hendra, Spechtrochim. Acta, Part A 25 (1969) 909.

[11] G.E. Mitchell, M.A. Henderson, J.M. White, J. Phys. Chem. 91 (1987) 3808.

[12] H. Froitzheim, U. Köhler, H. Lammering, Surf. Sci. 149 (1985) 537.

[13] L.J. Bellamy, The Infra-red Spectra of Complex Molecules, Wiley, New York, 1966.

[14] H. Ibach, D.L. Mills, Electron Energy Loss Spectroscopy and Surface Vibrations, Academic Press, New York, 1982.

[15] D.C. McKean, G. Davidson, L.A. Woodward, Spectrochim. Acta, Part A 26 (1970) 1815.

[16] C.H. van Dyke, E.W. Kifer, G.A. Gibbon, Inorg. Chem. 11 (1972) 408.

[17] A.A. Aquino, T.S. Jones, Appl. Surf. Sci. 104–105 (1996) 304.

[18] J. Yoshinobu, H. Tsuda, M. Onchi, M. Nishijima, Chem. Phys. Lett. 130 (1986) 170.

[19] Y. Bu, J.C.S. Chu, M.C. Lin, Surf. Sci. 285 (1993) 243.

[20] P.J. Chen, M.L. Colaianni, R.M. Wallace, J.T. Yates Jr., Surf. Sci. 244 (1991) 177.

[21] D.C. McKean, G.P. McQuillan, J. Mol. Struct. 63 (1980) 173.

[22] M.J.S. Dewar, E.G. Zoebisch, E.F. Healy, J.J.P. Stewart, J. Am. Chem. Soc. 107 (1985) 3902.

[23] N.C. Baird, M.J.S. Dewar, J. Chem. Phys. 50 (1969) 1262.

[24] M.J.S. Dewar, Haselbach, J. Am. Chem. Soc. 92 (1970) 590.

[25] R.C. Bingham, M.J.S. Dewar, D.H. Lo, J. Am. Chem. Soc. 97 (1975) 1285.

[26] V.A. Zayetz, CLUSTER-Z1 Quantum Chemical Software, Institute of Surface Chemistry, National Academy of Sciences of Ukraine, Kiev, 1990.

[27] V.D. Khavryutchenko Jr., A.V. Khavryutchenko, DYQU-AMOD Dynamical Quantum Modeling Software for Personal Computers, Joint Institute for Nuclear Researches,, Dubna, 1993. and Institute of Surface Chemistry, National Academy of Sciences of Ukraine, Kiev.

[28] V.G. Zavodinsky, I.A. Kuyanov, Appl. Surf. Sci. 141 (1999) 193.

[29] V.G. Zavodinsky, I.A. Kuyanov, E.N. Chukurov, Eur. Phys. J. B 6 (1998) 273.

[30] R.J. Hamers, Y. Wang, J. Shan, Appl. Surf. Sci. 107 (1996) 25.

[31] Y. Wang, X. Chen, R.J. Hamers, Phys. Rev. B 50 (1994) 4534.

[32] K.K. Chattarjee, J.R. During, S. Bell, J. Mol. Struct. 265 (1992) 25.

[33] K.D. Brommer, M. Needel, B.E. Larson, J.D. Joannopoulos, Phys. Rev. Lett. 68 (1992) 1355.

[34] G.L. Gutsev, V.K. Gryaznov, V.A. Nasluzov, Chem. Phys. 154 (1991) 291.